



Exothermic process of cast-in-place pile foundation and its thermal agitation of the frozen ground under a long dry bridge on the Qinghai-Tibet Railway*

Ya-ping WU^{†1,2}, Jian GUO^{†‡1}, Chun-xiang GUO², Wei MA³, Xiao-jun WANG¹

(¹School of Civil and Architecture Engineering, Ningbo Institute of Technology, Zhejiang University, Ningbo 315100, China)

(²School of Civil Engineering, Lanzhou Jiaotong University, Lanzhou 730070, China)

(³State Key Laboratory of Frozen Soil Engineering, Cold and Arid Regions Environment and Engineering Research Institute, Chinese Academy of Sciences, Lanzhou 730000, China)

[†]E-mail: yapingwu58@126.com; guoj@vip.163.com

Received Mar. 14, 2009; Revision accepted June 4, 2009; Crosschecked Dec. 15, 2009

Abstract: A number of dry bridges have been built to substitute for the roadbed on the Qinghai-Tibet Railway, China. The aim of this study was to investigate the exothermic process of cast-in-place (CIP) pile foundation of a dry bridge and its harm to the stability of nearby frozen ground. We present 3D heat conduction functions of a concrete pile and of frozen ground with related boundaries. Our analysis is based on the theory of heat conduction and the exponent law describing the adiabatic temperature rise caused by hydration heat. Results under continuous and initial conditions were combined to establish a finite element model of a CIP pile-frozen ground system for a dry bridge under actual field conditions in cold regions. Numerical results indicated that the process could effectively simulate the exothermic process of CIP pile foundation. Thermal disturbance to frozen ground under a long dry bridge caused by the casting temperature and hydration heat of CIP piles was substantial and long-lasting. The simulated thermal analysis results agreed with field measurements and some significant rules relating to the problem were deduced and conclusions reached.

Key words: Exothermic process of hydration heat, Cast-in-place (CIP) pile foundation, Dry bridge, Thermal agitation, Frozen ground, Qinghai-Tibet Railway

doi:10.1631/jzus.A0900522

Document code: A

CLC number: U23

1 Introduction

In the construction of the Qinghai-Tibet Railway, China to avoid problems caused by frost heave and thaw-settlement of frozen ground, dry bridge structures with a total length of more than 70 km were built to substitute for the roadbed in regions where frozen ground is warmer and ice-rich (Fig. 1) (Huang and Wu, 2004).

Cast-in-place (CIP) pile foundations, being of high bearing capacity and easy to build, were widely used for supporting dry bridges on the Qinghai-Tibet Railway. Because of the length of the bridges (3–12 km), however, the casting temperature and hydration heat caused by the CIP pile foundation may cause significant thermal agitation of the permafrost and endanger the stability of frozen ground. As a result, the strength of the frozen ground and the bearing capacity of the piles may be heavily reduced.

To reduce these risks, it is important to investigate and forecast the exothermic process of hydration heat of CIP pile foundation and its effects on frozen ground by field testing or numerical methods.

[‡] Corresponding author

* Project supported by the National Natural Science Foundation of China (No. 50678076), and the Opening Foundation of the State Key Laboratory of Frozen Soil Engineering (No. SKLFSE200603), China
 © Zhejiang University and Springer-Verlag Berlin Heidelberg 2010



Fig. 1 A dry bridge on the Qinghai-Tibet Railway

At present, relevant laws of hydration heat release of cement have been established mainly on the basis of adiabatic temperature rise. These laws include empirical formulas which have been adapted to epoxy and polyester polymer concrete (Vipulanandan and Paul, 1990), an exponent law relevant to the case of large dam concrete (Liu, 2001; Xiang and Yang, 2003) and a hyperbola law which considers the chemical reaction rate of concrete (Zhang *et al.*, 2003).

In studies related to hydration heat acting on frozen ground, Liu *et al.* (2002) studied the redistribution of the temperature field of an artificial ice wall affected by heat of concrete hydration using an exponent law of hydration heat release and a finite element method. Ma and Wang (2003) ignored the exothermic process of a signal concrete pile (and assumed that the temperature of frozen ground remained constant along the length of the pile) to establish a simple model of stable state heat transfer for a monolayer cylinder using the law of conservation of heat. The model can be used to calculate the thermal agitation range of a signal concrete pile to frozen ground. Wu *et al.* (2006) ignored the exothermic process of concrete and assumed that the temperature rise due to hydration heat can be treated as the adiabatic temperature rising acting on the wall of pile holes. They assumed this to analyze the refreezing process of ground for a concrete pile group base of a bridge in permafrost.

With respect to numerical simulation of temperature fields in frozen ground engineering, presently, many related research reports have been published (Comini, 1974; Li *et al.*, 1998; Lai *et al.*, 2003a;

2003b), most concentrating on the subgrade and tunnel engineering without considering effects of actual field temperature, casting temperature of concrete and hydration heat.

The research reports on the pile foundation in permafrost are mainly focused on the time-dependent mechanical behavior of a loaded pile (Nixon, 1990; Stelizer and Andersland, 1991; Foriero and Ladanyi, 1995; Biggar *et al.*, 1996; Wu *et al.*, 2005; 2007; Yu *et al.*, 2007).

To date, there has been a lack of relevant research reports on the numerical simulation of the exothermic process of hydration heat caused by CIP pile foundations in frozen ground and its thermal agitation of the frozen ground under a long dry bridge.

In this paper, aimed at the above problems, we present 3D heat conduction functions of a concrete pile and those of frozen ground with related boundaries. Our analysis is based on the theory of heat conduction and the exponent law describing the adiabatic temperature rise caused by hydration heat. Results under continuous and initial conditions were combined to establish a finite element model of a CIP pile-frozen ground system. For a dry bridge structure under actual field conditions on the Qinghai-Tibet Railway, the liberation process of CIP pile foundation and its thermal disturbance to the nearby frozen ground were calculated and analyzed, and recommendations were made. For the time variation of soil temperature, numerical results from this study corresponded with those from field tests (Huang and Wu, 2004), demonstrating the external validity of the methodology in the current study.

2 Calculating model and general parameters

We considered the Yamaer River Dry Bridge on the Qinghai-Tibet Railway as an analytic example. The bridge was assembled by 92 equal simple spans with a total length of 7.36 km. A single span is 8 m in length. The beam of the bridge is supported by the pier with a transverse beam and two CIP piles (Fig. 1).

Considering symmetry, we selected No. 14 pier as a calculation model, in which the axes distance between two piles is 3.3 m. The pile is 1 m in diameter and 19.8 m in length, of which 18 m is buried beneath

the ground. The quarter calculating model (Fig. 2) is 40 m in length (vertical to the bridge line), 4 m (half of a span) in width (along the bridge line) and 40 m in thickness of the frozen soil (permafrost base is about 40 m in depth).

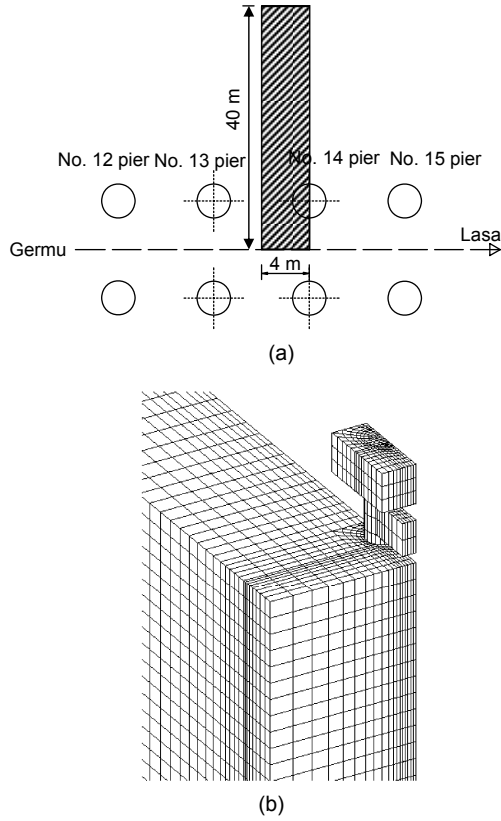


Fig. 2 Quarter calculating model considering symmetry
(a) Range of calculating model (dash area); (b) Quarter calculating model of the pier with abutment

3 Heat conduction equations of a concrete pile

In the initial stage of the casting, the speed of the concrete heat release is much larger than that of heat conduction, so the temperature rising due to the hydration heat can be treated as the adiabatic temperature rise. In the calculation process, the concrete adiabatic temperature rise with different casting temperatures and ages can be expressed as (Liu, 2001)

$$\xi = \xi_u (1 - e^{-mt}), \quad (1)$$

where ξ_u denotes the maximum adiabatic temperature rise ($^{\circ}\text{C}$), m is a temperature attenuation parameter changing with the brand of the cement and casting temperature ($1/d$), for casting temperature being 5°C , $m=0.295/d$ (Liu, 2001), and t is the concrete age (d).

In the computing process, the concrete of Cement+DZ series offered by the laboratory of the 12th Bureau Consortium of Chinese Railway is adopted. The maximum adiabatic temperature rising can be expressed as

$$\xi_u = \frac{M_1 Q}{\sum_{i=1}^6 M_i C_i}, \quad (2)$$

where Q denotes the hydration heat of cement, for Portland cement, $Q=313$ kJ/kg (Liu, 2001). The subscripts i ($=1, 2, \dots, 6$) respectively denote the ordering of the cement, sand, carpolite, admixture, cementing materials and water. M_i denotes the consumption of the i th material; C_i is the heat capacity of the i th material.

When a coordinate system is established by vertical axis z and horizontal axes x, y , a 3D heat conduction equation of concrete is

$$C_c \frac{\partial T_c}{\partial t} = \frac{\partial}{\partial x} \left(\lambda_c \frac{\partial T_c}{\partial x} \right) + \frac{\partial}{\partial y} \left(\lambda_c \frac{\partial T_c}{\partial y} \right) + \frac{\partial}{\partial z} \left(\lambda_c \frac{\partial T_c}{\partial z} \right) + Q_{\xi}, \quad (3)$$

where T_c , C_c , λ_c respectively denote the temperature, volume heat capacity and thermal conductivity of the concrete; Q_{ξ} denotes the unit volume heat flow rate of the concrete ($\text{J}/(\text{m}^3 \cdot \text{h})$), and

$$Q_{\xi} = C_c \frac{d\xi}{dt} = C_c \xi_u m e^{-mt}. \quad (4)$$

The initial conditions are

$$T(y, r, t)|_{t=0} = T_{co} \quad (\text{within } \Omega_c), \quad (5)$$

where $C_c=2300$ ($\text{kJ}/(\text{m}^3 \cdot ^{\circ}\text{C})$) denotes the volumetric heat capacity of the concrete, T_{co} denotes the casting temperature of the concrete, and Ω_c is the field of the concrete.

On the interface between concrete pile and frozen soil, the continuous condition of the temperature and condition of the energy conservation are given respectively by

$$T_c = T_s, \quad (6)$$

$$\lambda_c \frac{\partial T_c}{\partial n} - \lambda_s \frac{\partial T_s}{\partial n} = 0, \quad (7)$$

where T_s denotes the frozen soil temperature.

4 Heat conduction equations of frozen ground

The coefficient of the heat conductivity and specific heat of the frozen ground vary with temperature. The frozen ground will release or absorb enormous latent heat when it thaws or freezes. So the effect of the phase-change latent heat should be considered in this problem.

For the calculating model shown in Fig. 1, the coefficient of the heat conductivity in each orientation is assumed to be a constant. 3D heat conduction equation can be expressed:

within Ω_f , $T_s = T_f$ and

$$C_f \frac{\partial T_f}{\partial t} = \frac{\partial}{\partial x} \left(\lambda_r \frac{\partial T_f}{\partial x} \right) + \frac{\partial}{\partial y} \left(\lambda_r \frac{\partial T_f}{\partial y} \right) + \frac{\partial}{\partial z} \left(\lambda_r \frac{\partial T_f}{\partial z} \right), \quad (8)$$

within Ω_u , $T_s = T_u$ and

$$C_u \frac{\partial T_u}{\partial t} = \frac{\partial}{\partial x} \left(\lambda_u \frac{\partial T_u}{\partial x} \right) + \frac{\partial}{\partial y} \left(\lambda_u \frac{\partial T_u}{\partial y} \right) + \frac{\partial}{\partial z} \left(\lambda_u \frac{\partial T_u}{\partial z} \right), \quad (9)$$

where T_f , C_f and λ_f denote, respectively, the frozen ground temperature, volumetric heat capacity and thermal conductivity in the freezing zone Ω_f . The subscript 'u' is the corresponding magnitudes in the thawing zone.

Another initial condition is

$$T_s(x, y, z, t)|_{t=0} = T_{s0}, \quad (10)$$

where T_{s0} denotes the initial soil temperature obtained

from the field measured data. The fixed boundary conditions can be expressed as follows:

$$\lambda \frac{\partial T}{\partial n} = h(T_a - T), \text{ on ground surface,} \quad (11)$$

$$\frac{\partial T}{\partial n} = 0, \text{ on side face,} \quad (12)$$

$$\frac{\partial T}{\partial n} = 0.029 \text{ }^\circ\text{C/m, on bottom surface,} \quad (13)$$

where h denotes the convective heat transfer coefficient between air and ground surface; T_a denotes the temperature on the add-surface (Zhu, 1988), and

$$T_a = T_{av} + At + 12.2 \sin \left(\frac{2\pi}{8640} t + \frac{4\pi}{3} \right). \quad (14)$$

In Eq. (14) T_{av} denotes the average temperature on the add-surface; A denotes the future rate of air temperature rise; t is time, h.

On the movable phase-change interface $\xi(t)$, the temperature continuous and energy conservation conditions are given by

$$T_u(\xi(t)) = T_f(\xi(t)) = T_m, \quad (15)$$

$$\lambda_r \frac{\partial T_f}{\partial n} - \lambda_u \frac{\partial T_u}{\partial n} = L\rho_d(\theta_w - \theta_u) \frac{d\xi(t)}{dt}, \quad (16)$$

where T_m is the freezing temperature; L is the phase-change latent heat of the water; θ_w presents the water content; θ_u denotes the unfrozen-water content; ρ_d denotes the dry density.

The phase-change process is calculated using the method of sensible-heat-capacity. It is assumed that phase-change takes place in a temperature range ($T_m \pm \Delta T$). The expressions for the heat capacity C_s and heat conductivity coefficient λ_s are given, respectively, by

$$C_s = \begin{cases} C_f, & T < T_m - \Delta T, \\ \frac{L\rho_d(\theta_w - \theta_u)}{2\Delta T} + \frac{C_f + C_u}{2}, & T_m - \Delta T \leq T \leq T_m + \Delta T, \\ C_u, & T > T_m + \Delta T, \end{cases} \quad (17)$$

$$\lambda_s = \begin{cases} \lambda_r, & T < T_m - \Delta T, \\ \lambda_r + \frac{\lambda_u - \lambda_r}{2\Delta T} [T - (T_m - \Delta T)], & T_m - \Delta T \leq T \leq T_m + \Delta T, \\ \lambda_u, & T > T_m + \Delta T. \end{cases} \quad (18)$$

So Eqs. (8) and (9) can be simplified as follows:

$$C_s \frac{\partial T_s}{\partial t} = \frac{\partial}{\partial x} \left(\lambda_s \frac{\partial T_s}{\partial x} \right) + \frac{\partial}{\partial y} \left(\lambda_s \frac{\partial T_s}{\partial y} \right) + \frac{\partial}{\partial z} \left(\lambda_s \frac{\partial T_s}{\partial z} \right). \quad (19)$$

5 Calculating method of the pile-soil system

The coefficient of the heat conductivity and specific heat of the frozen ground vary with the temperature and the phase interface is not fixed, so the energy conservation conditions on the interface are nonlinear, and analytic results for this problem cannot be obtained. We adopt the finite element method to solve the problem.

Using the separation Galerkin method, a finite element equation of the 3D heat conduction problem is deduced from Eqs. (3) and (19), and then a global thermal equilibrium equation of the CIP pile-frozen ground system can be obtained:

$$\mathbf{K}\mathbf{T}_t + \mathbf{M} \frac{d}{dt} \mathbf{T}_t = \mathbf{p}_t, \quad (20)$$

where \mathbf{K} denotes the temperature stiffness matrix, \mathbf{M} denotes the non-steady-state changing-temperature matrix, \mathbf{T} denotes the column vector of unknown temperature values, and \mathbf{p} the temperature load column vector associated with the boundary conditions. The subscript t denotes the time, and we have

$$\mathbf{K} = \sum \left[\int_{\Omega_e} \lambda \left(\frac{\partial}{\partial x} \mathbf{N}^T \frac{\partial}{\partial x} \mathbf{N} + \frac{\partial}{\partial y} \mathbf{N}^T \frac{\partial}{\partial y} \mathbf{N} + \frac{\partial}{\partial z} \mathbf{N}^T \frac{\partial}{\partial z} \mathbf{N} \right) d\Omega + \int_{S_e} h \mathbf{N}^T \mathbf{N} ds \right], \quad (21)$$

$$\mathbf{M} = \sum \int_{\Omega} C \mathbf{N}^T \mathbf{N} d\Omega, \quad (22)$$

$$\mathbf{p}_t = \sum \int_{\Omega} \mathbf{N}^T Q_o d\Omega + \int_{S_e} h T_a \mathbf{N}^T ds, \quad (23)$$

where Ω_e and S_e denote, respectively, the field and perimeter of the element, and \mathbf{N} denotes the shape function matrix.

In the time range, adopting the Crank-Nicolson difference format, we can express Eq. (20) as

$$\left(\mathbf{K} + \frac{2\mathbf{M}}{\Delta t} \right) \mathbf{T}_t = (\mathbf{p}_t - \mathbf{p}_{t-\Delta t}) + \left(\frac{2\mathbf{M}}{\Delta t} - \mathbf{K} \right) \mathbf{T}_{t-\Delta t}. \quad (24)$$

Considering that C and λ are associated with temperature, the results for this equation can be obtained by adopting a suitable time step and iteration precision.

6 Results and analyses

According to the actual field conditions in the building site of No. 14 pier of the Yamaer River Dry Bridge (Huang and Wu, 2004), the annual average air temperature and average temperature on the add-surface were -5°C and -1°C , respectively, the air temperature rising rate $A=2.28 \times 10^{-6}^\circ\text{C/h}$, and the frozen ground temperature grades was 0.029°C/m .

The casting temperature of CIP pile foundation was 5°C . For per cubic meter concrete, the cement of 337.8 kg was used.

The mix proportion of concrete used in the CIP pile was: cement:admixture:flyash:sand:carpolite:water=1:0.125:0.125:2.137:3.082:0.533, and from Eq. (2), we can obtain $\xi_u=51.2^\circ\text{C}$.

The measured hydrology-geology data and thermal parameters are listed in Table 1 (Huang and Wu, 2004).

In the computation, the frozen ground temperature measured in the building site and casting temperature of the concrete (here is 5°C) were adopted as initial conditions.

According to the numerical results predicted by the finite element method model, Fig. 3 shows the time variation curves of the temperature below the ground in pile center, pile edge and pile side 20 cm, respectively.

From Fig. 3, characteristics of the exothermic process of CIP pile foundations are noted:

1. The value of the casting temperature (here at 5°C) formed the initial value of the temperature rise in the pile center. The values of the temperature rise in

Table 1 Hydrology-geology data and heat parameters*

Depth under ground (m)	Material	ρ_d (kg/m ³)	θ_w (%)	c_u (kJ/(m ³ ·°C))	C_f (kJ/(m ³ ·°C))	λ_u (kJ/(m·h·°C))	λ_f (kJ/(m·h·°C))
0–0.5	Grit stone	2500	13	3186.3	2310.5	10.4397	10.7352
0.5–1.5	Fat sand soil	2000	15	3353.3	2377.5	9.9217	10.6386
1.5–2.0	Mudstone	2500	17.03	3522.8	2445.5	9.4294	10.5429
2–3	Mudstone	2500	17.5	3562.3	2461.3	7.0670	10.0169
3–5	Mudstone	2500	27.8	4422.7	2806.3	7.9581	10.2302
5.0–14.2	Mudstone	2500	22	3938.0	2612.0	8.7363	10.4011
14.4–19.1	Mudstone	2500	20	3771.0	2545.0	8.3736	10.3231
19.4–25.3	Mudstone	2500	15.5	3395.0	2394.3	9.4294	10.5429
8.9–9.1; 14.2–14.4; 19.1–19.4; 20.6–20.8; 24.0–24.2; 25.0–25.3	Ice layer contained soil	1000	96	4014.9	2023.0	2.1553	8.1132

* The parameters of reinforced concrete are: $\rho_d=2500$ kg/m³, $c_u=2300.0$ kJ/(m³·°C), $C_f=2300.0$ kJ/(m³·°C), $\lambda_u=6.264$ kJ/(m·h·°C), $\lambda_f=6.264$ kJ/(m·h·°C)

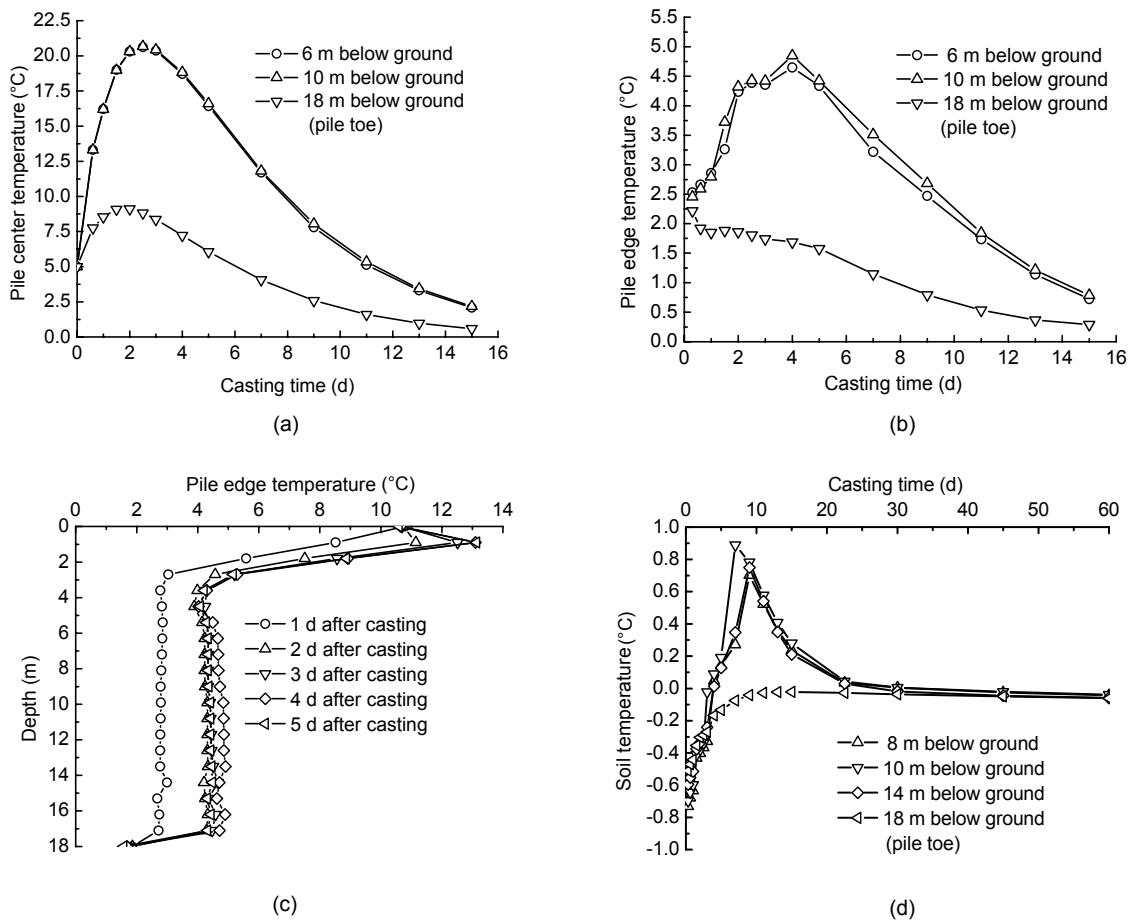


Fig. 3 Temperature of pile foundation predicted using the finite element method model

(a) Time variation of temperature in pile center; (b) Time variation of temperature at pile edge; (c) Temperature along depth of pile foundation vs. time; (d) Time variation of soil temperature on the pile side

the pile center were larger than those at the pile edge. The peak value of the temperature in the pile center occurred at 2.5th day after casting, and that at the edge occurred at 4.2th day after casting. The difference in the peak temperature from the center to the edge was 16 °C (Figs. 3a and 3b).

2. Because of the air temperature acting, the pile edge temperatures nearby the ground surface was higher than elsewhere (Fig. 3c).

3. Because of the pile toe directly contacting the frozen ground, the temperature at the pile toe was lower than elsewhere (Figs. 3c and 3d).

4. The soil temperature on the pile side 20 cm reached about 0.9 °C in the 7th day after casting, whereafter it decreased and came to 0 °C. This result agrees with the field observation results and confirms the validity of our methodology (Fig. 3d).

In this study, the parameter of refreezing rate was used to evaluate the degree of hydration heat agitating the frozen ground, which is defined as the ratio of the temperature of disturbed frozen ground to that of undisturbed frozen ground at an equal depth of the pile foundation. If the temperature of disturbed frozen ground becomes positive, the refreezing rate is zero.

Fig. 4 shows the variation of the refreezing rate at the pile edge and that in the middle of a span vs. casting time. The average of refreezing rate along the depth of the foundation was defined as the average refreezing rate. The curves of the average refreezing rate vary with casting time and are shown in Fig. 5. From Fig. 4, it can be seen that, because of the influence of air temperature on ground surface and that of frozen ground on the pile toe, the refreezing rates of frozen ground surrounding the pile distributed nonuniformly along the depth of the foundation, and in most instances, the refreezing rates near the earth surface and pile toe were larger than those elsewhere, but this difference decreased with the time. Furthermore, the soil temperature around the pile perimeter gradually reduced and the refreezing rate gradually increased with time. In the middle of a span, however, the soil temperature gradually increased and the refreezing rate gradually decreased in the first year and then was reversed, gradually conforming to the variation of the refreezing rate around the pile perimeter in the latter years. This illustrates that the hydration heat had transferred from the pile group

perimeter to the middle of the span (the half span sport). Thus, the temperature of the frozen ground in the middle of a span firstly began to increase, reached a maximum value about 1 year later, and then began to decrease. The temperature reducing process in the half span sport was 1 year later than that near the pile perimeter. After 3 years, the average refreezing rates became constant. After 7 years, the average refreezing rate reached 93.25% (Fig. 5).

According to above analyses, the hydration heat caused by the CIP pile foundation could bring significant thermal agitation of the permafrost and endanger the stability of frozen ground under a dry bridge.

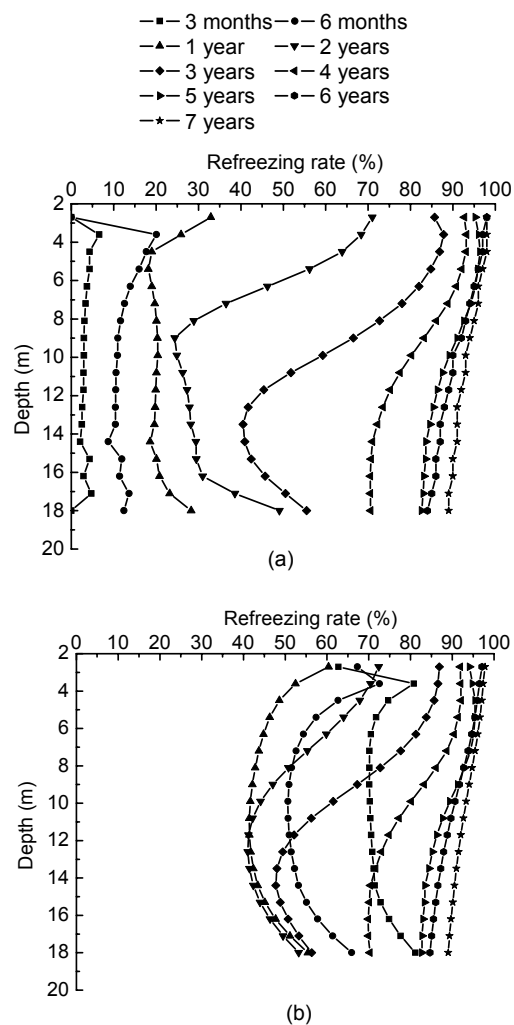


Fig. 4 Refreezing rate along depth of pile foundation vs. casting time predicted using the finite element method model (a) In the pile edge; (b) In the middle of a span

Figs. 6a and 6b show the temperature along the depth of the frozen soil in the middle of a span after casting 167 d and that in the undisturbed region after casting 240 d, respectively. From the figures we can see that, for calculated values and field measured

values (Huang and Wu, 2004), affected by the climatic change, the values above 3 m (active layer above permafrost) are difficult to compare, and below 3 m the calculated values and field measured value preferably fit close. This suggests that the computing method of this study is reliable.

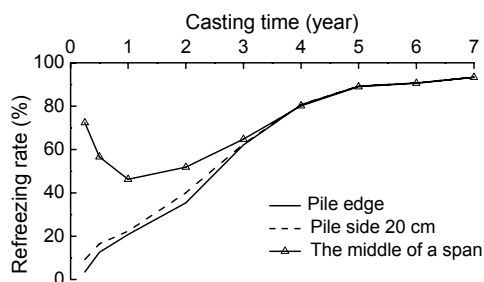
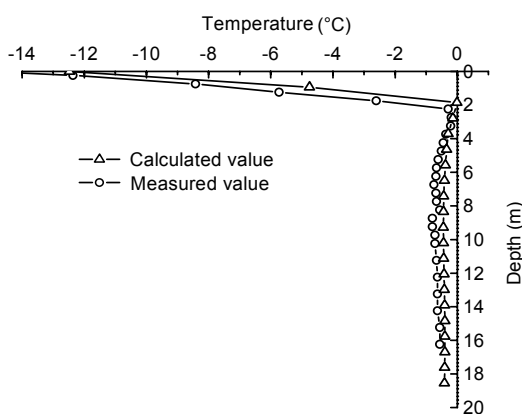
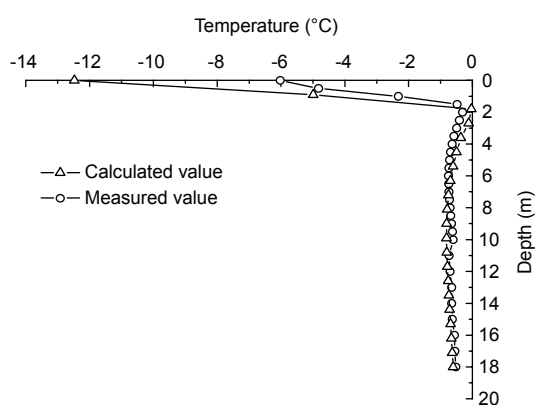


Fig. 5 Time variation of the average refreezing rate predicted using the finite element method model



(a)



(b)

Fig. 6 Comparison of calculated values and measured values of temperature field

(a) Temperature in the middle of a span after casting 167 d; (b) Temperature in the undisturbed region after casting 240 d

7 Conclusion

1. The method of this study can effectively simulate the exothermic process of CIP pile foundation and change event of soil temperature field around the pile and nearby in permafrost under the actual field conditions in cold regions, which provides a way for analyzing similar problems. The analysis can provide references for the theoretical investigation and construction design of CIP pile foundations in cold regions.

2. Thermal disturbance to frozen ground under a long dry bridge caused by the casting temperature and hydration heat of CIP piles was substantial and long-lasting, which can form a warming frozen ground region under a dry bridge, and endanger the stability of frozen ground. By reducing casting temperature and employing more low heat of hydration cement, the thermal disturbance to frozen ground can be reduced.

3. The method used in this study can not only be used to calculate the temperature field of CIP pile foundation of bridges in permafrost, but also be used to calculate that of other buildings in permafrost, and has preferable theoretical and applied costs.

References

Biggar, K.W., Sego, D.C., Stahl, R.P., 1996. Long-term pile load testing system performance in saline and ice-rich permafrost. *Journal of Cold Regions Engineering, ASCE*, **10**(3):149-162. [doi:10.1061/(ASCE)0887-381X(1996)10:3(149)]

Comini, G., 1974. Finite element solution of nonlinear heat conduction problems with special reference to phase change. *International Journal for Numerical Methods in Engineering*, **35**(8):613-624. [doi:10.1002/nme.1620080314]

Foriero, A., Ladanyi, B., 1995. FEM simulation of interface problem for laterally loaded piles in permafrost. *Cold Regions Science and Technology*, **23**(2):121-136. [doi:10.1016/0165-232X(94)00008-L]

- Huang, D.F., Wu, Y.P., 2004. Research on the Stability of Pile Foundation of Dry Bridge and Its Temperature Field. Research Report No. 003, Qinghai-Tibet Railway Corporation, p.65-69 (in Chinese).
- Lai, Y.M., Li, J.J., Niu, F.J., Yu, W.B., 2003a. Nonlinear thermal analysis of Qing-Tibet railway embankments in cold regions. *Journal of Cold Regions Engineering, ASCE*, **17**(4):171-184. [doi:10.1061/(ASCE)0887-381X(2003)17:4(171)]
- Lai, Y.M., Wu, Z.W., Zhang, S.J., Yu, W.B., Den, Y.S., 2003b. Study of methods to control frost action in cold regions tunnels. *Journal of Cold Regions Engineering, ASCE*, **17**(4):144-152. [doi:10.1061/(ASCE)0887-381X(2003)17:4(144)]
- Li, D.Q., Wu, Z.W., Zhu, L.N., 1998. Heat stability analysis of embankment of the degrading permafrost district of Changshitou Mountain in the East of Tibetan Plateau, China. *Cold Regions Science and Technology*, **28**(3):183-188. [doi:10.1016/S0165-232X(98)00018-4]
- Liu, B.J., 2001. Concrete Technology. People's Transportation Press, Beijing, China (in Chinese).
- Liu, J.S., Tang, J.C., Yang, J.J., 2002. Redistribution of temperature field of artificial ice wall affected by heat of concrete hydration. *Journal of China Coal Society*, **27**(5):517-520 (in Chinese).
- Ma, B.G., Wang, Y.F., 2003. Research on thermal effect to frozen earth groundwork produced by concrete engineering. *Hypothermia Building Technician*, (1):4-7 (in Chinese).
- Nixon, J.F., 1990. Effect of climatic warming on pile creep in permafrost. *Journal of Cold Regions Engineering, ASCE*, **4**(1):67-73. [doi:10.1061/(ASCE)0887-381X(1990)4:1(67)]
- Stelizer, D.L., Andersland, O.B., 1991. Model pile-settlement behavior in frozen sand. *Journal of Cold Regions Engineering, ASCE*, **5**(1):1-13.
- Vipulanandan, C., Paul, E., 1990. Epoxy and polyester polymer concrete. *Materials Journal, American Concrete Institute*, **87**(3):241-251.
- Wu, Y.P., Zhu, Y.L., Guo, C.X., Su, Q., Ma, W., 2005. Multi-field coupling model and its applications for pile foundation in permafrost. *Science in China Series D-Earth Sciences*, **48**(7):968-977. [doi:10.1360/082004-175]
- Wu, Y.P., Su, Q., Guo, C.X., Zhu, Y.L., Zhang, L.X., Zhao, S.Y., 2006. Nonlinear analysis of refreezing process of ground for concrete pile group base of bridge in permafrost. *China Civil Engineering Journal*, **39**(2):8-12 (in Chinese).
- Wu, Y.P., Shu, C.S., Ma, W., Sun, J.Z., Peng, W.W., 2007. Study of the load transfer curves of steel pipe pile in frozen ground. *Journal of Glaciology and Geocryology*, **29**(1):21-25.
- Xiang, M., Yang, C.J., 2003. Study of the hydro-thermal dissipation law of high strength concrete. *Concrete*, (3):27-30 (in Chinese).
- Yu, Z.Q., Wang, X., Jiang, D.J., 2007. Experimental Study on Bearing Features of Bored Pile under Non-refreezing Condition in Permafrost Region. International Conference on Transportation Engineering, p.3882-3884.
- Zhang, Z.M., Song, H.T., Huang, H.Y., 2003. New theory on adiabatic temperature rise and heat conduction equation of concrete. *Journal of Hehai University*, **30**(3):1-6 (in Chinese).
- Zhu, L.N., 1988. Study for add-surfaces of different underlying surfaces in plateau permafrost region. *Journal of Glaciology and Geocryology*, **10**(1):35-39.